

## Supporting Information

### Advantages of Molecular Weight Identification during Native MS

#### Screening

Ahad Khan<sup>1</sup>, Anne Bresnick<sup>2</sup>, Sean Cahill<sup>2</sup>, Mark Girvin<sup>2</sup>, Steve Almo<sup>2</sup>, Ronald Quinn<sup>1</sup>

#### Affiliations

<sup>1</sup>Griffith Institute for Drug Discovery, Griffith University, Brisbane, Australia

<sup>2</sup>Albert Einstein College of Medicine, NY, USA

#### Correspondence

*Prof. Ronald J. Quinn*

Griffith Institute for Drug Discovery

Griffith University

Brisbane, QLD, 4111

Australia

Phone: +61 7 373 56006

Fax: +61 7 373 56001

r.quinn@griffith.edu.au

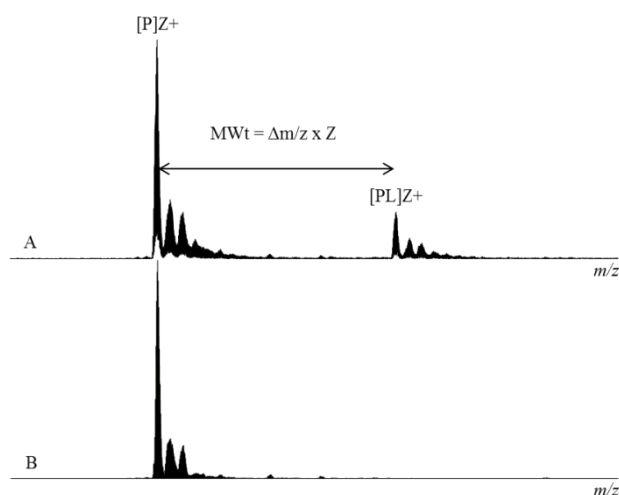


**Fig. 1S** Hit detection and molecular weight (MW) determination in ESI-FTMS screening. In **B**, the spectrum shows only a protein peak,  $[P]Z^+$ , and in **A**, the spectrum shows a protein peak,  $[P]Z^+$ , and a protein-ligand complex peak ( $[PL]Z^+$ ). Here,  $Z^+$  is the charge state of the protein in the positive ionization mode. MW of the ligand (hit) is calculated from the mass difference ( $\Delta m/z \times Z$ ).

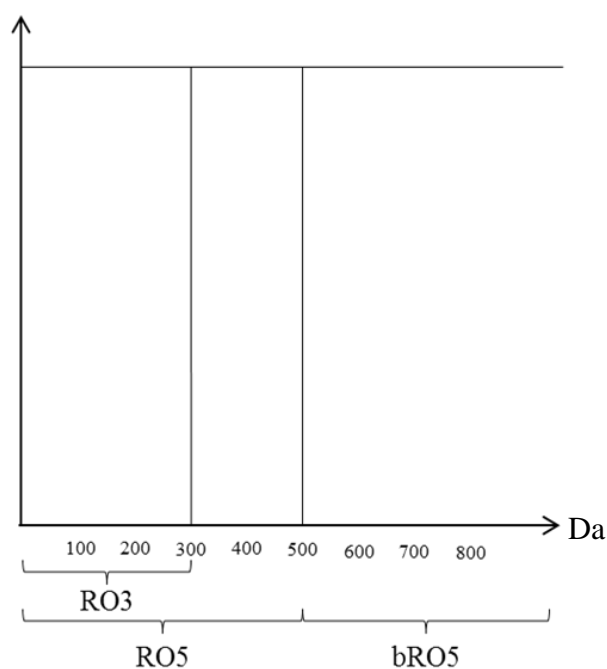


**Fig. 2S** Chemical subspaces of hits based on their molecular weights. The hits with a molecular weight  $< 300$  Da were categorized as lead-like compounds (RO3) and hits with a molecular weight  $< 500$  Da were categorized as drug-like compounds (RO5). The compounds with a molecular weight  $> 500$  Da were beyond the “rule of five” (bRO5).

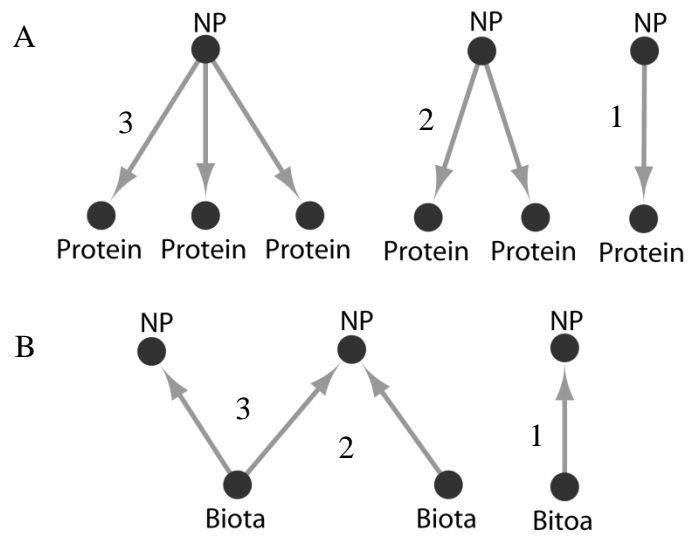


**Fig. 3S** Unique and common hits based on molecular weights. NP = natural product. The unique hits showed binding to only one protein (A1) and the common hits showed binding to more than one protein (A2 & A3). The hits (NP) were detected from one (B1) or multiple biota (B2) or multiple hits from one biota (B3).

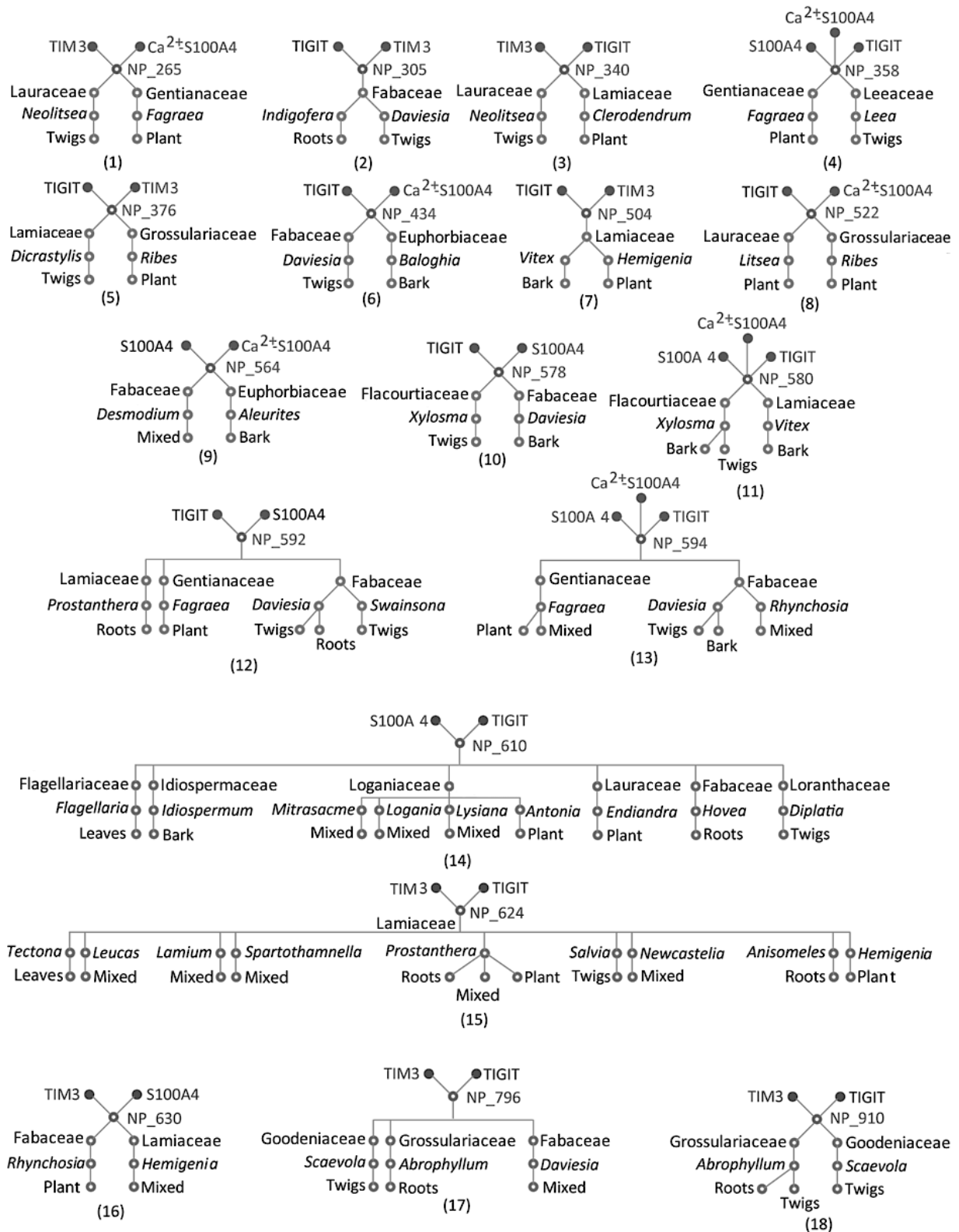


**Fig. 4S** Common hits and their taxonomical classes, parts of the plants used, and the proteins.

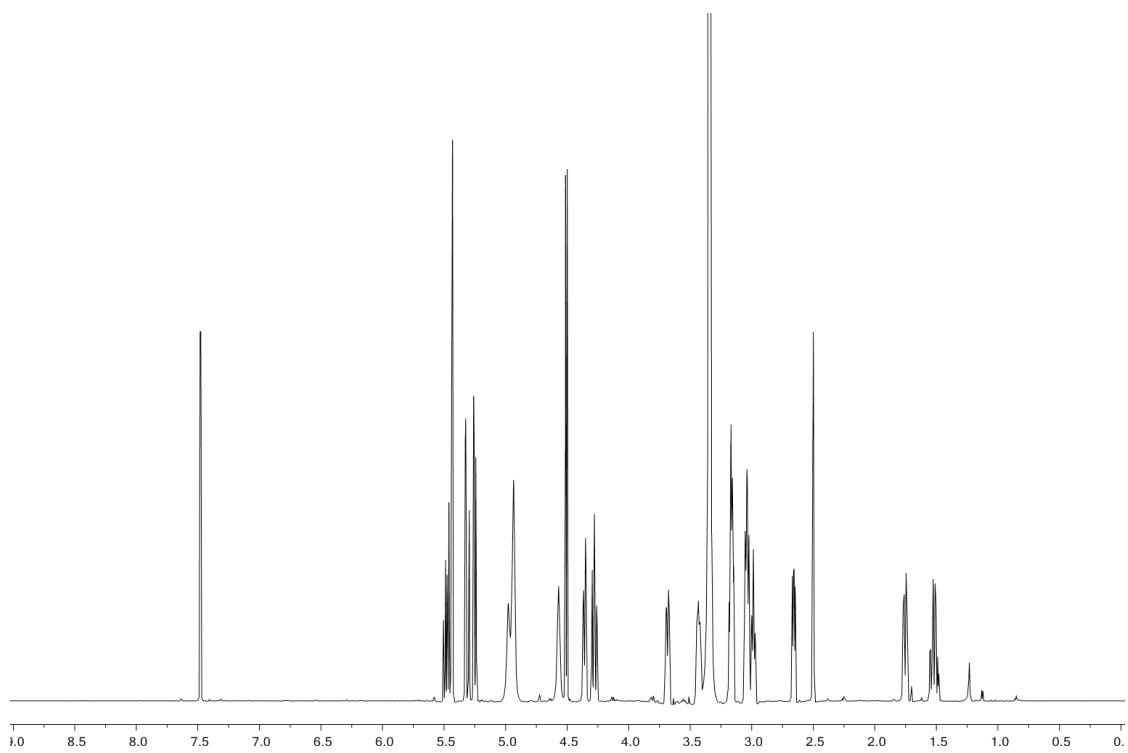


**Fig. 5S**  $^1\text{H}$ -NMR spectrum of NP\_358 acquired in  $\text{DMSO-}d_6$  (800 MHz).

**Fig. 6S**  $^{13}\text{C}$ -NMR spectrum of NP\_358 acquired in  $\text{DMSO-}d_6$  (800 MHz).

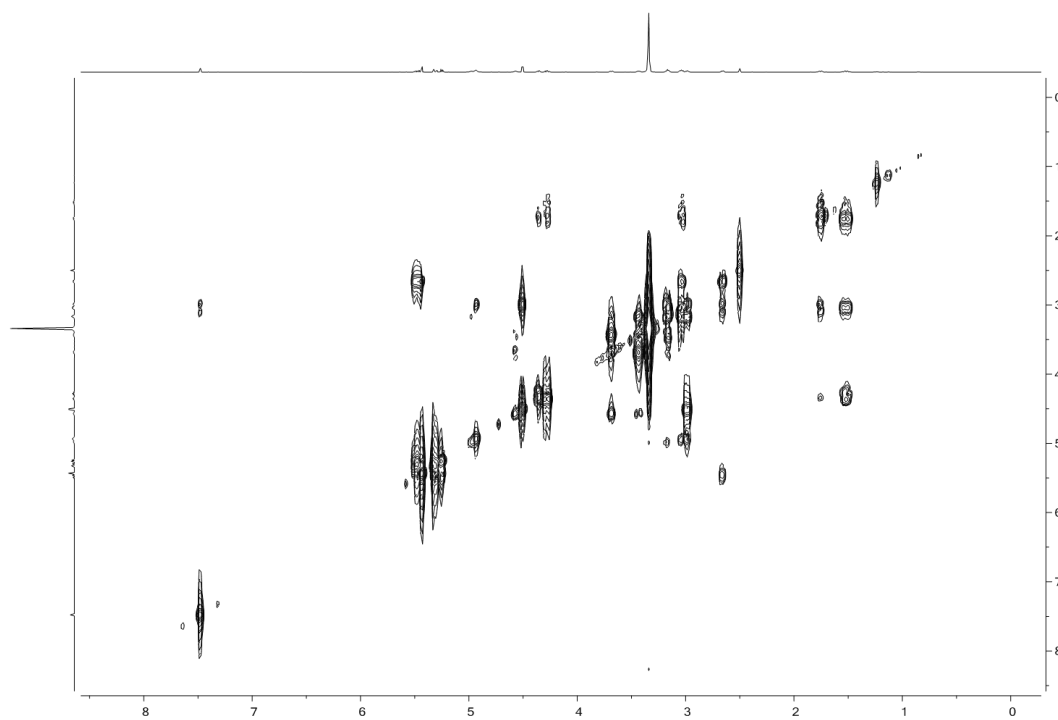


**Fig. 7S** gCOSY spectrum of NP\_358 acquired in DMSO-*d*<sub>6</sub> (800 MHz).

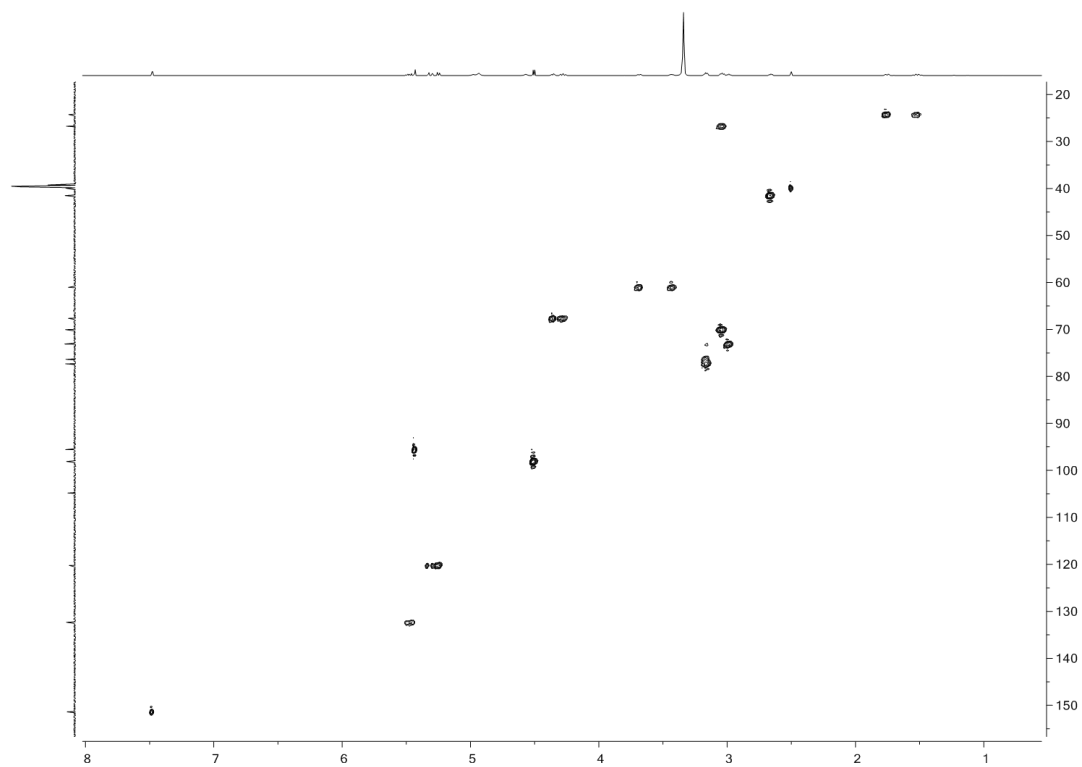


**Fig. 8S** HSQCAD spectrum of NP\_358 acquired in DMSO-*d*<sub>6</sub> (800 MHz).

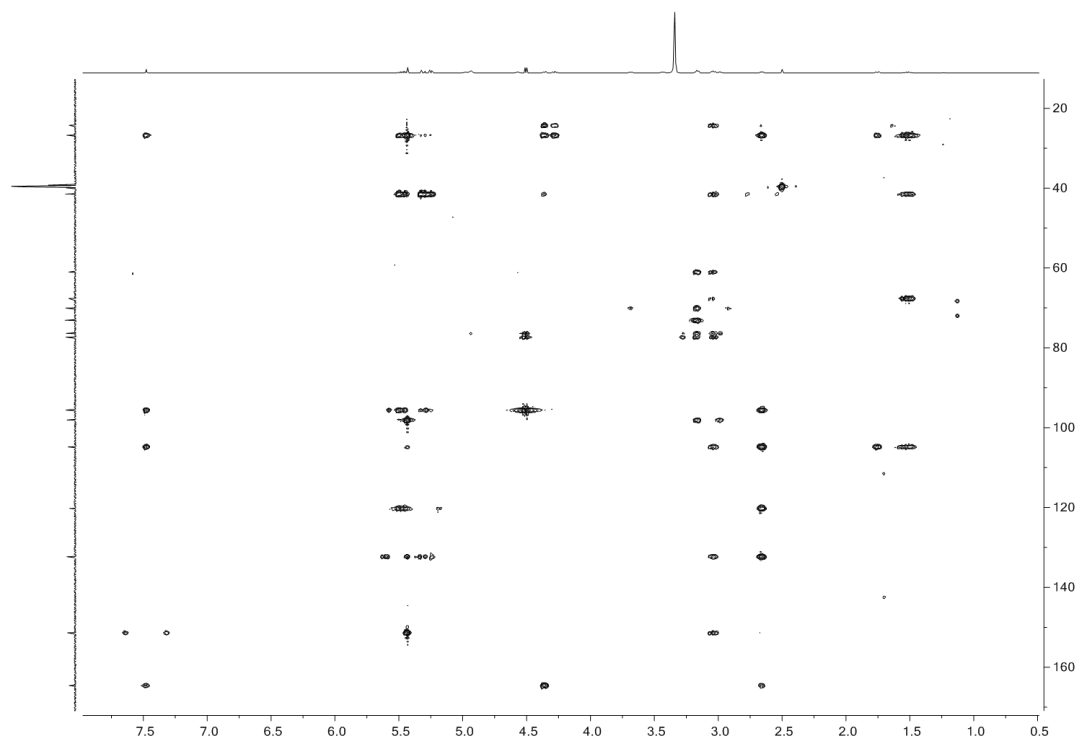


**Fig. 9S** HMBCAD spectrum of NP\_358 acquired in DMSO-*d*<sub>6</sub> (800 MHz).

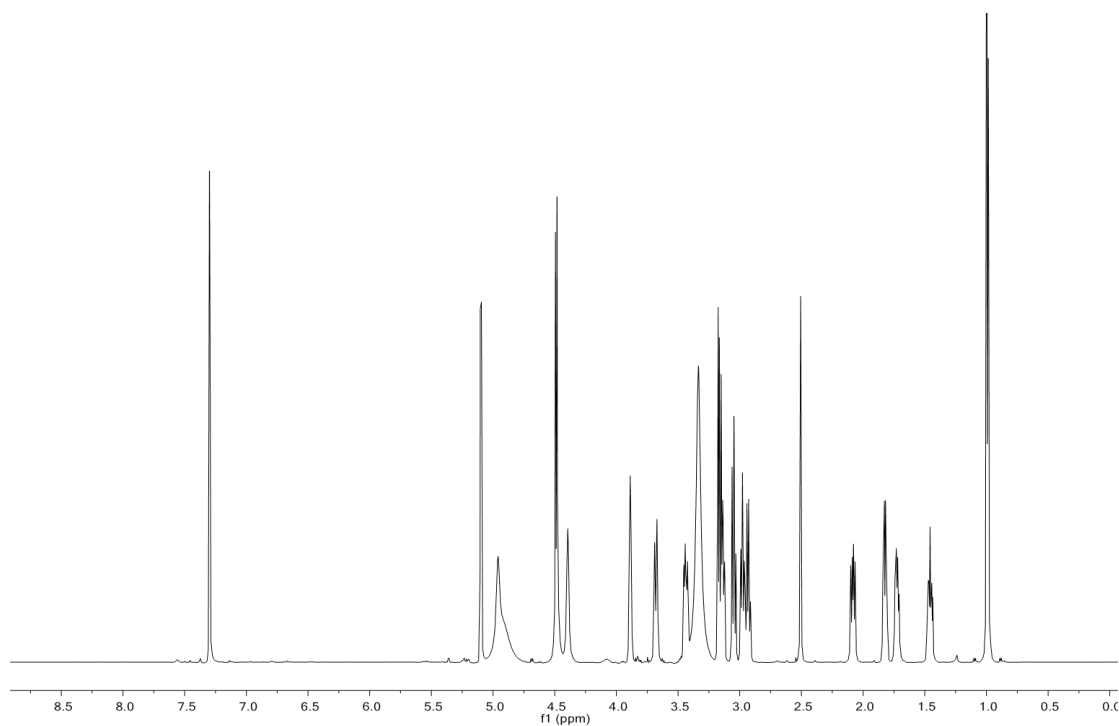


**Fig. 10S** <sup>1</sup>H-NMR spectrum of NP\_376 acquired in DMSO-*d*<sub>6</sub> (800 MHz).

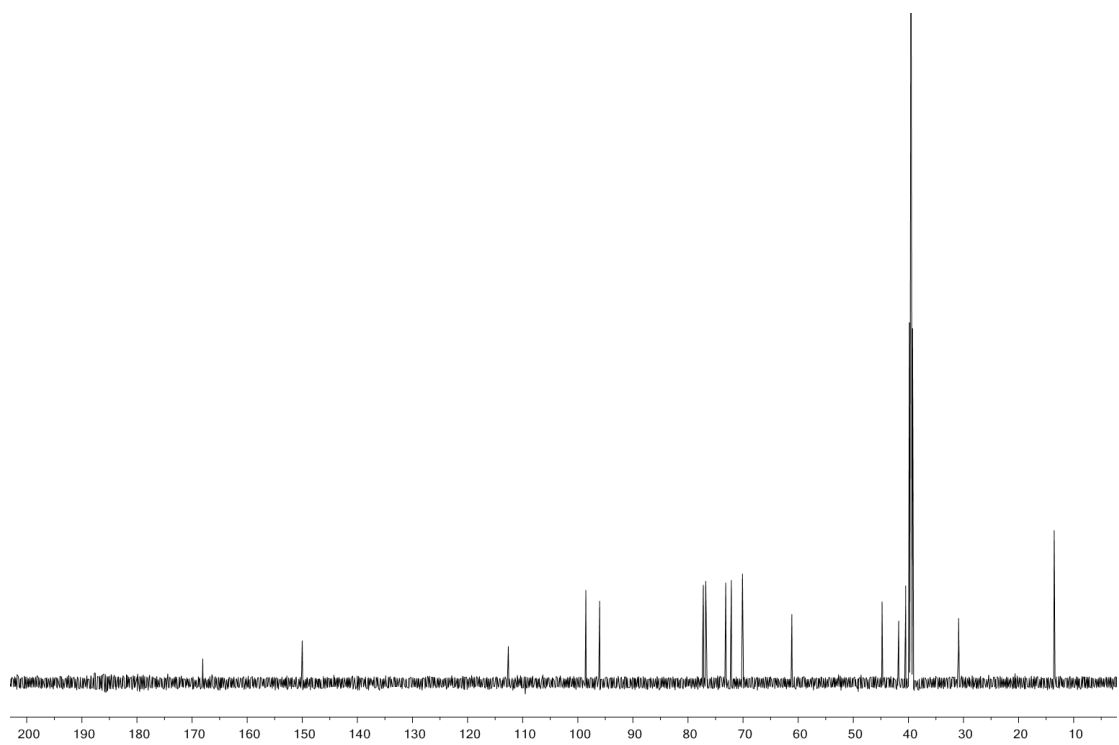


**Fig. 11S** <sup>13</sup>C-NMR spectrum of NP\_376 acquired in DMSO-*d*<sub>6</sub> (800 MHz).

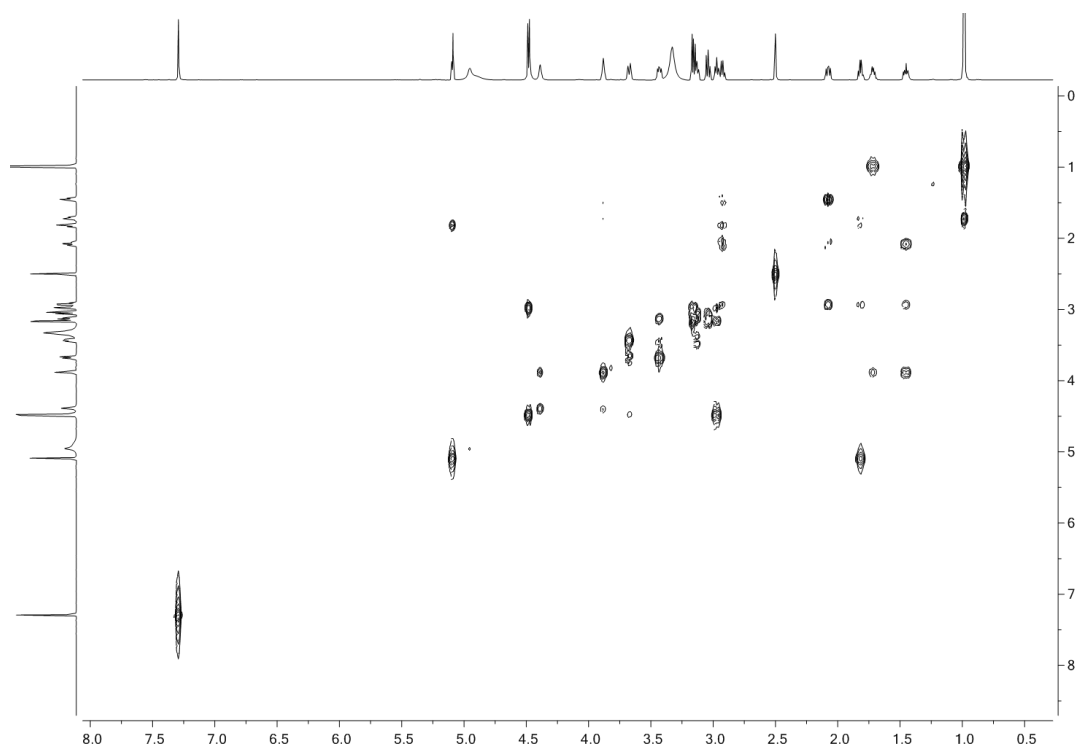


**Fig. 12S** gCOSY spectrum of NP\_376 acquired in DMSO-*d*<sub>6</sub> (800 MHz).

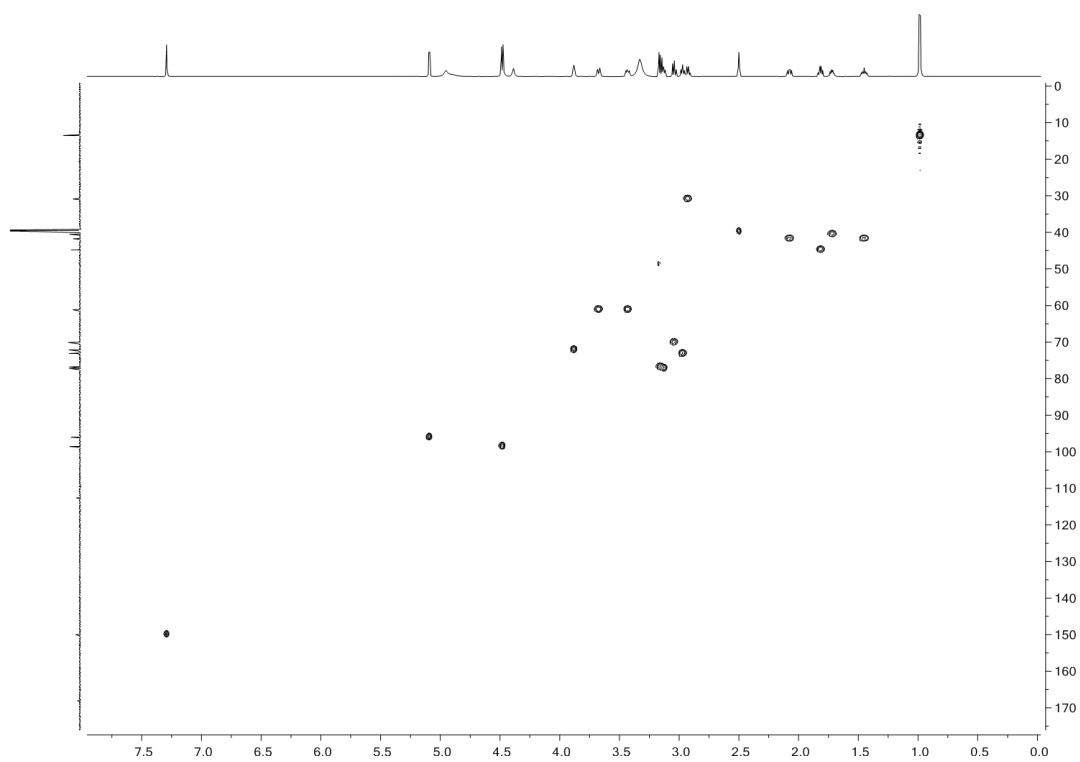


**Fig. 13S** HSQCAD spectrum of NP\_376 acquired in DMSO-*d*<sub>6</sub> (800 MHz).



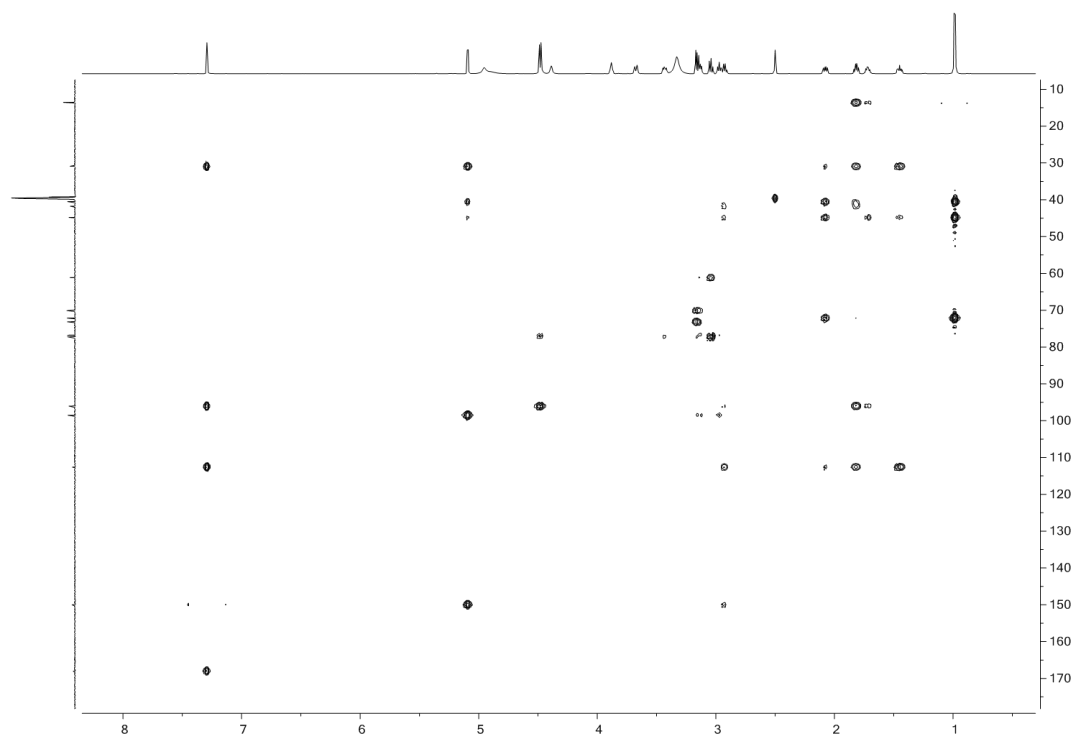


**Fig. 14S** HMBCAD spectrum of NP\_376 acquired in DMSO- $d_6$  (800 MHz).

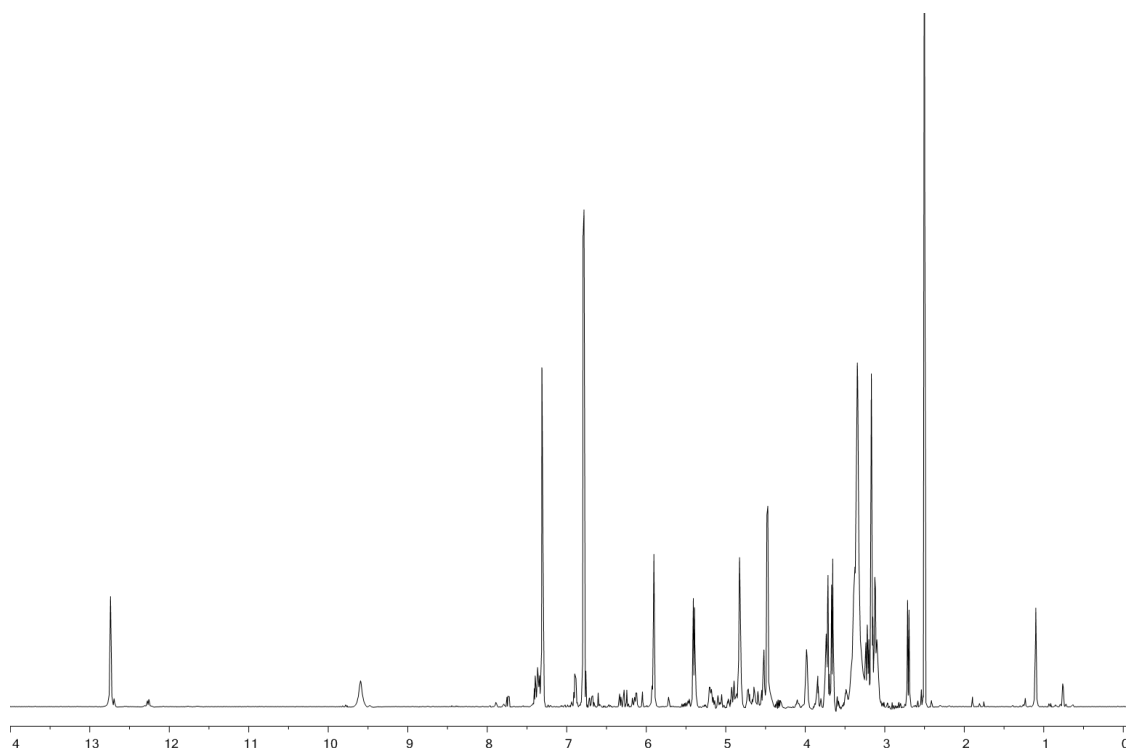


**Fig. 15S**  $^1\text{H}$ -NMR spectrum of NP\_434 acquired in DMSO- $d_6$  (800 MHz).

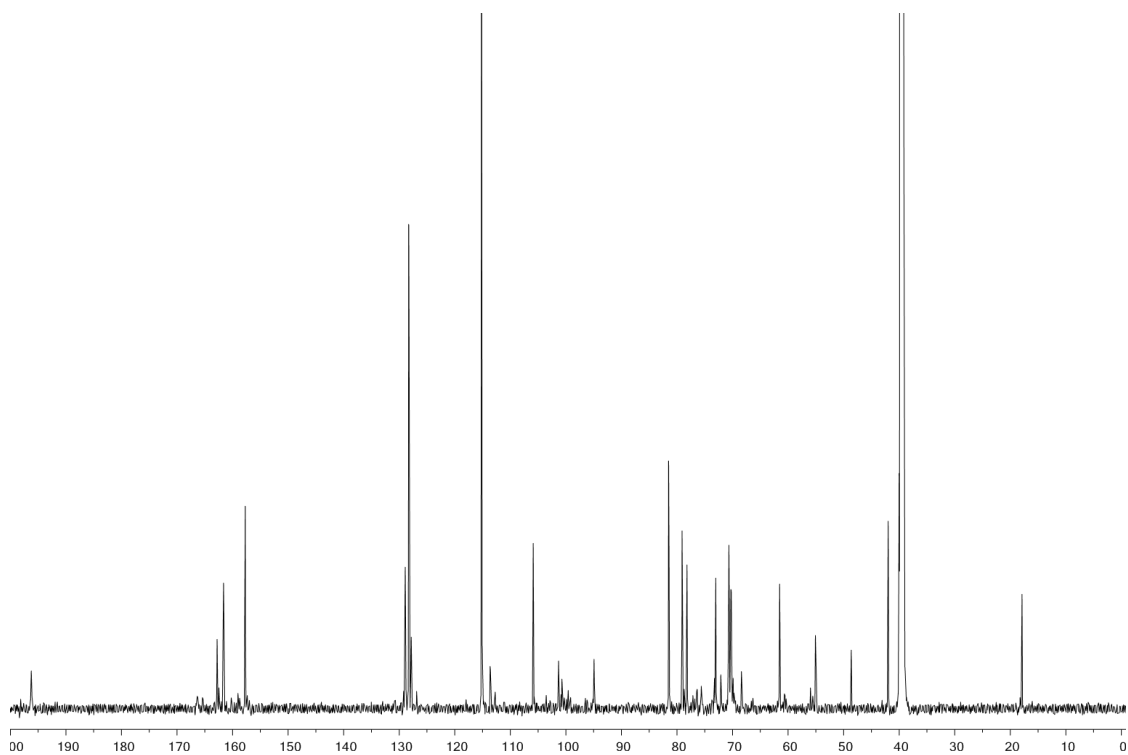


**Fig. 16S**  $^{13}\text{C}$ -NMR spectrum of NP\_434 acquired in DMSO- $d_6$  (800 MHz).

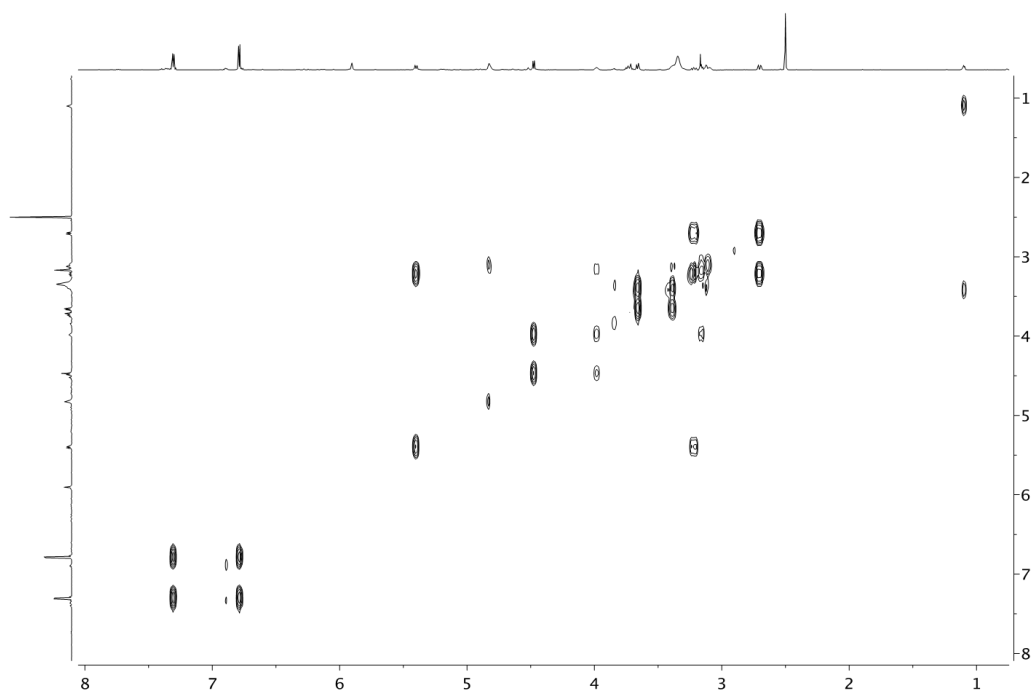


**Fig. 17S** gCOSY spectrum of NP\_434 acquired in DMSO- $d_6$  (800 MHz).

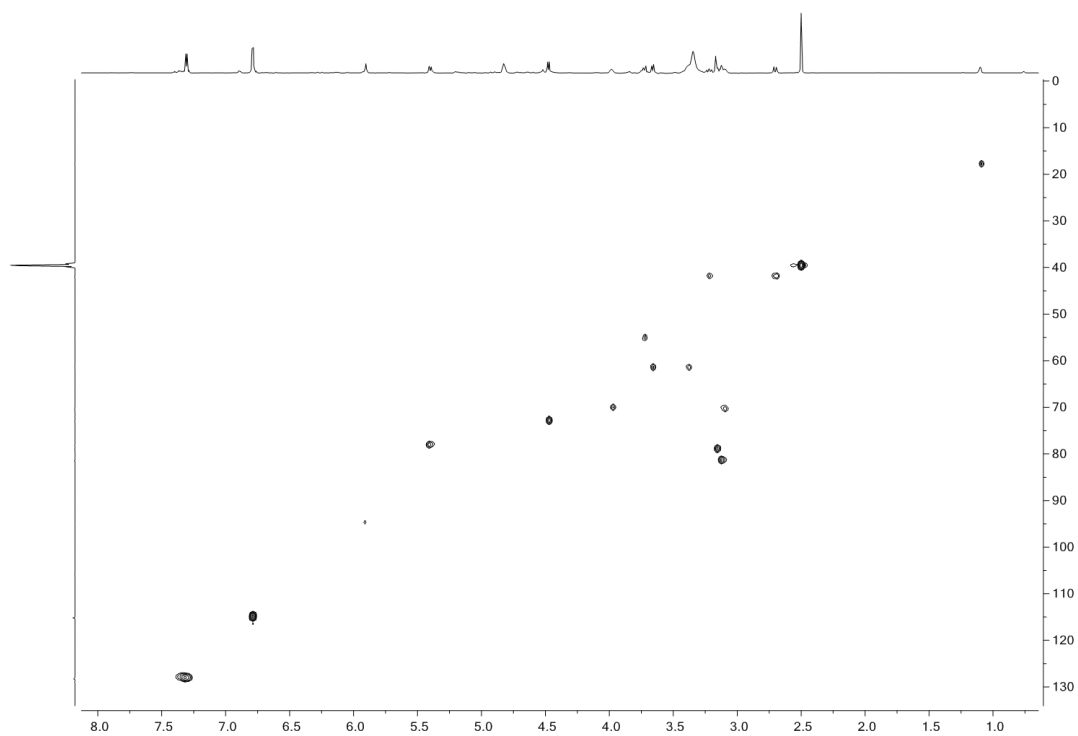


**Fig. 18S** HSQCAD spectrum of NP\_434 acquired in DMSO- $d_6$  (800 MHz).

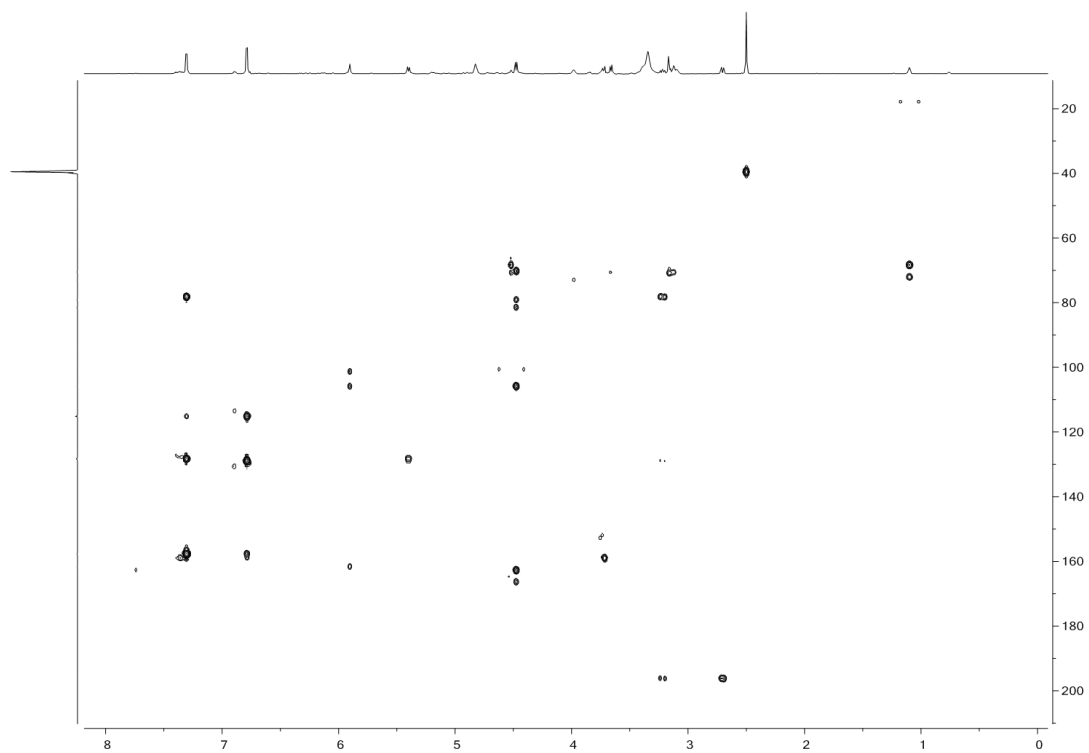


**Fig. 19S** HMBCAD spectrum of NP\_434 acquired in DMSO- $d_6$  (800 MHz).

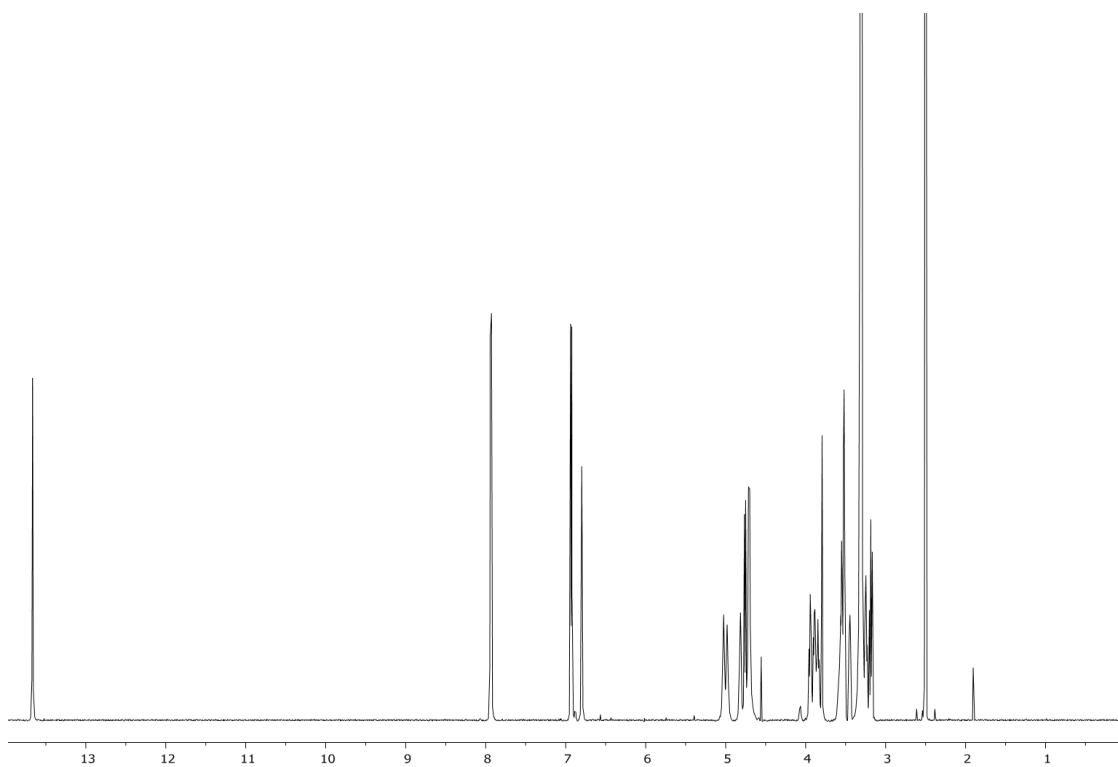


**Fig. 20S** <sup>1</sup>H-NMR spectrum of NP\_564 acquired in DMSO-*d*<sub>6</sub> (800 MHz).

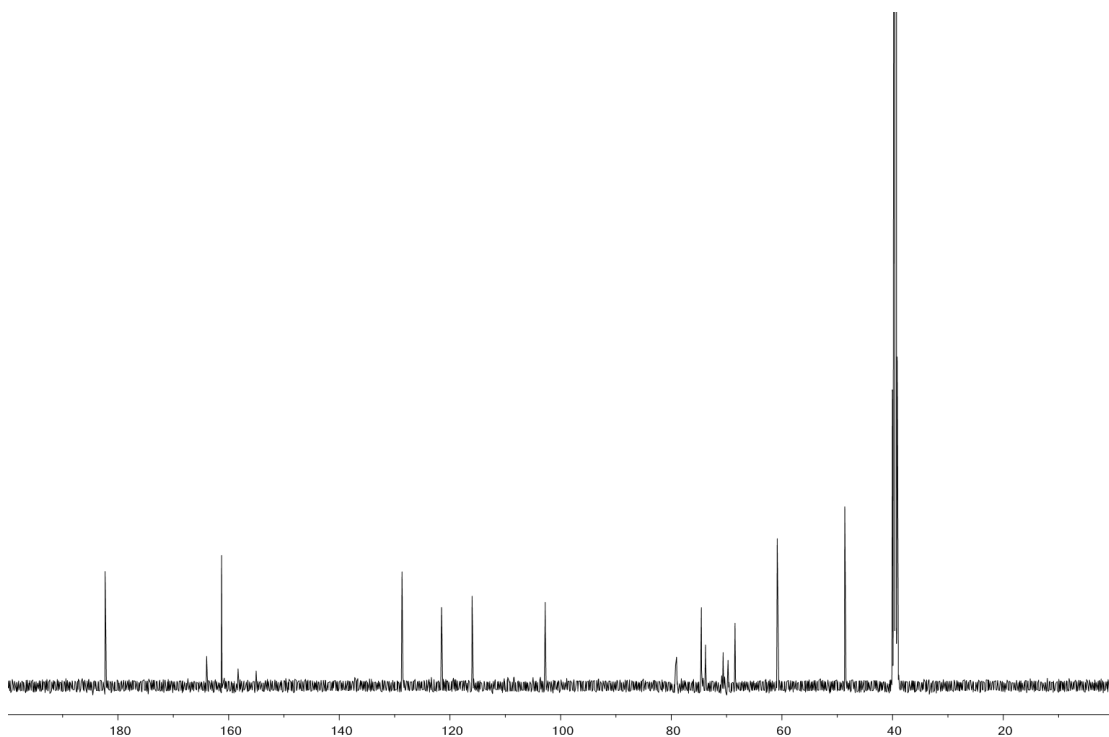


**Fig. 21S** <sup>13</sup>C-NMR spectrum of NP\_564 acquired in DMSO-*d*<sub>6</sub> (800 MHz).

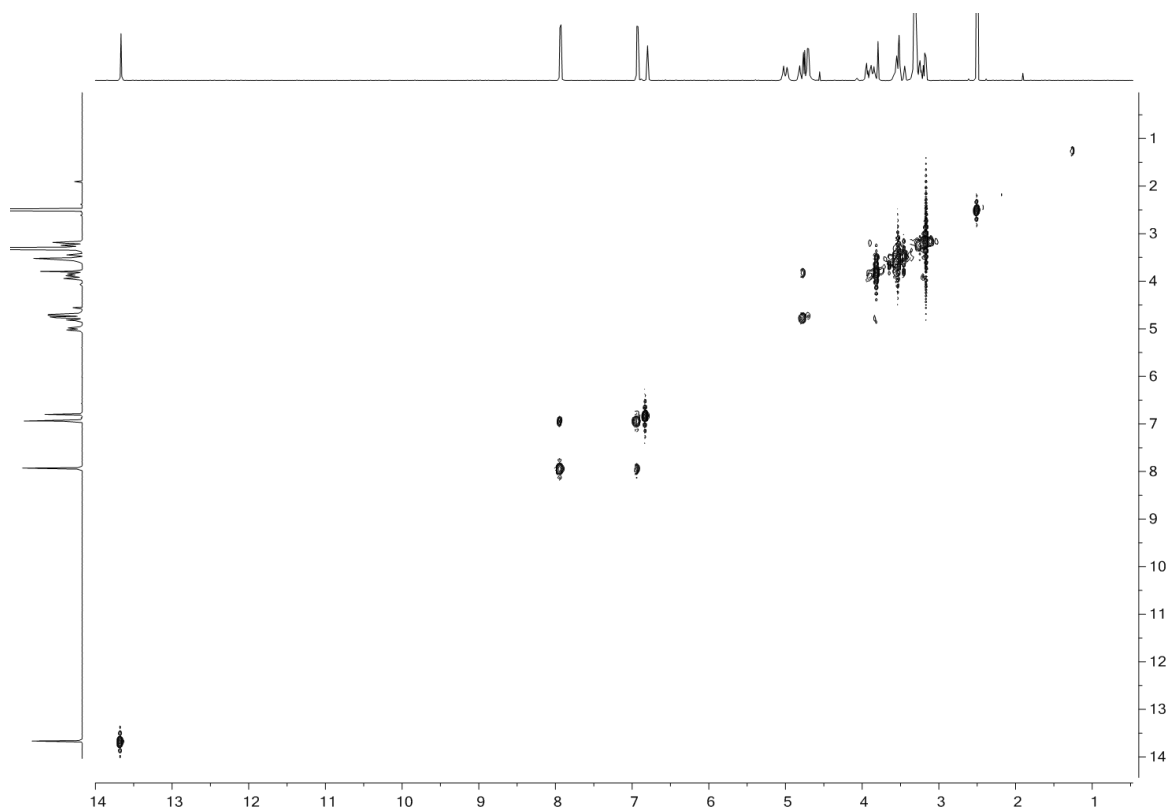


**Fig. 22S** gCOSY spectrum of NP\_564 acquired in DMSO-*d*<sub>6</sub> (800 MHz).

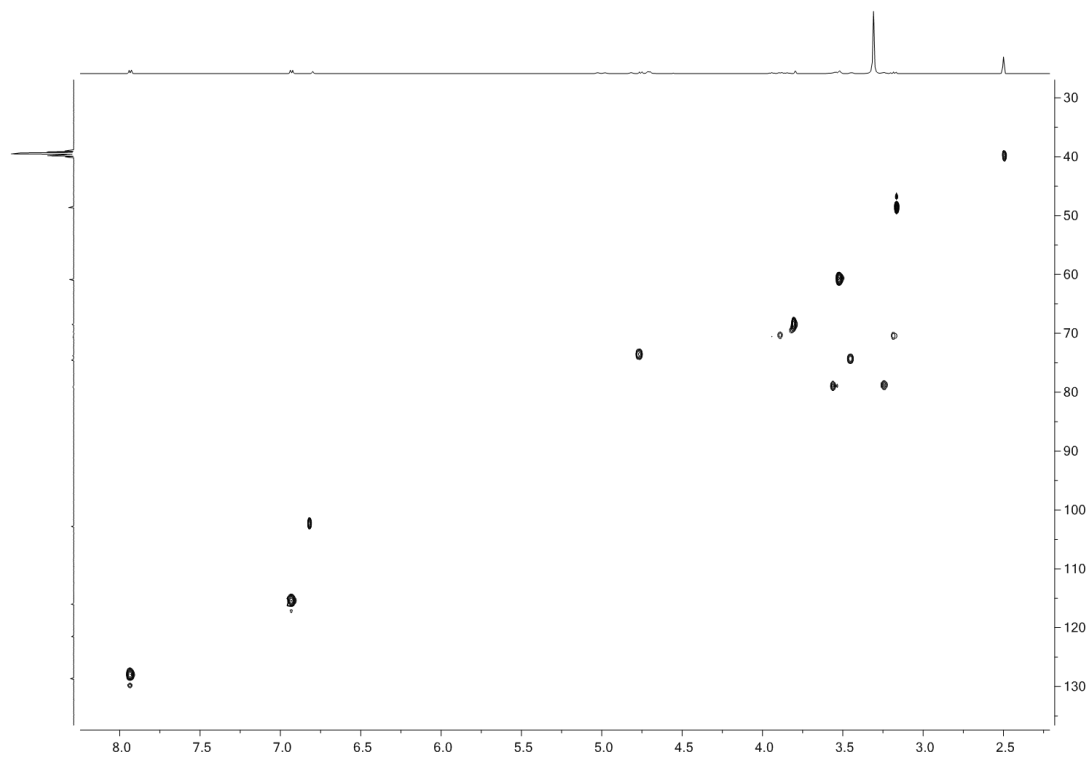


**Fig. 23S** HSQCAD spectrum of NP\_564 acquired in DMSO-*d*<sub>6</sub> (800 MHz).

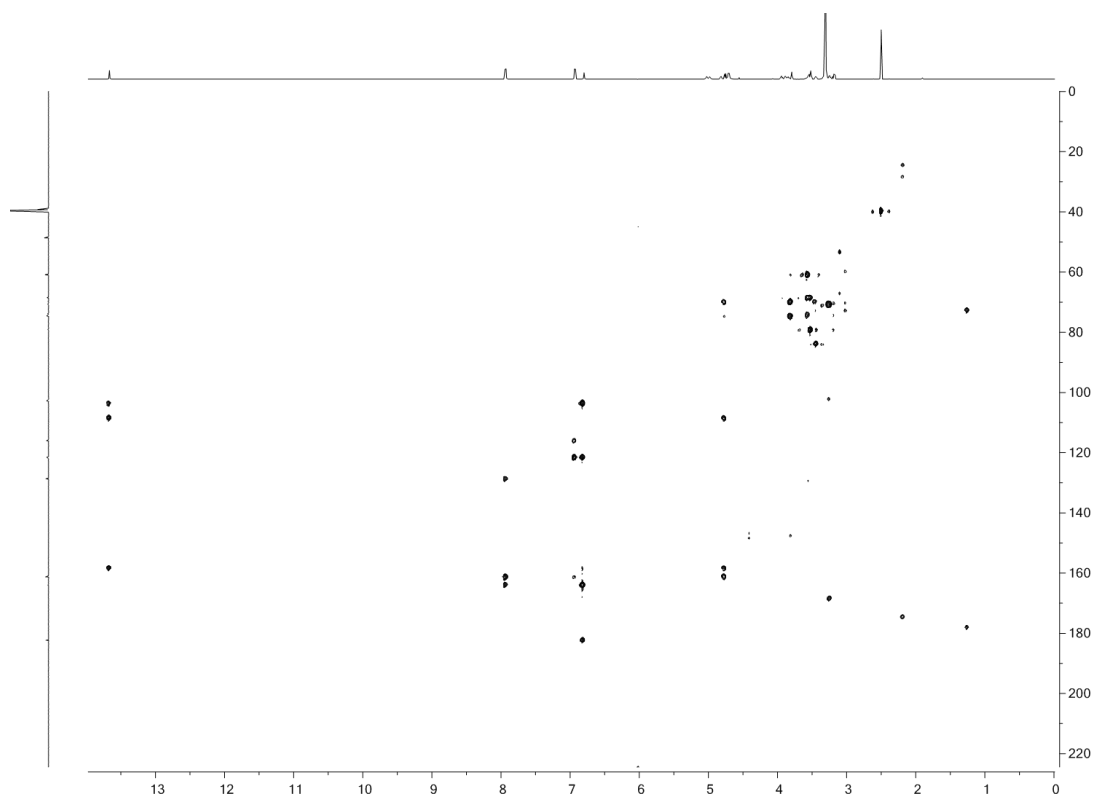


**Fig. 24S** HMBCAD spectrum of NP\_564 acquired in DMSO- $d_6$  (800 MHz).

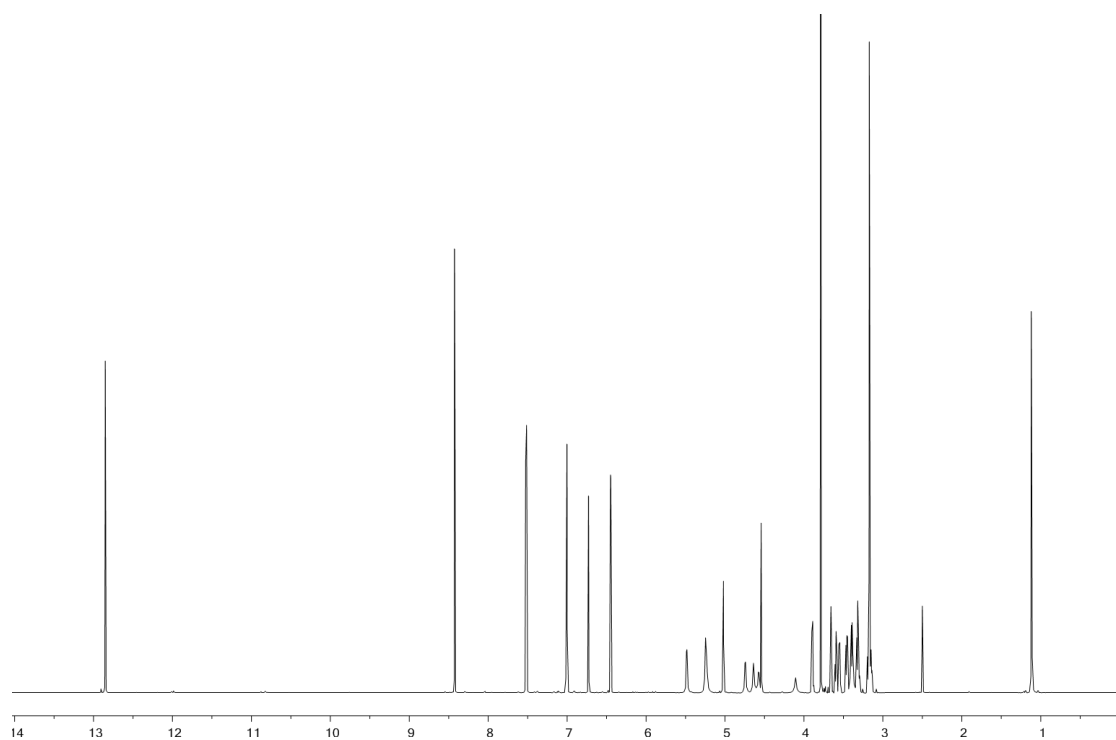


**Fig. 25S**  $^1\text{H}$ -NMR spectrum of NP\_592 acquired in DMSO- $d_6$  (800 MHz).

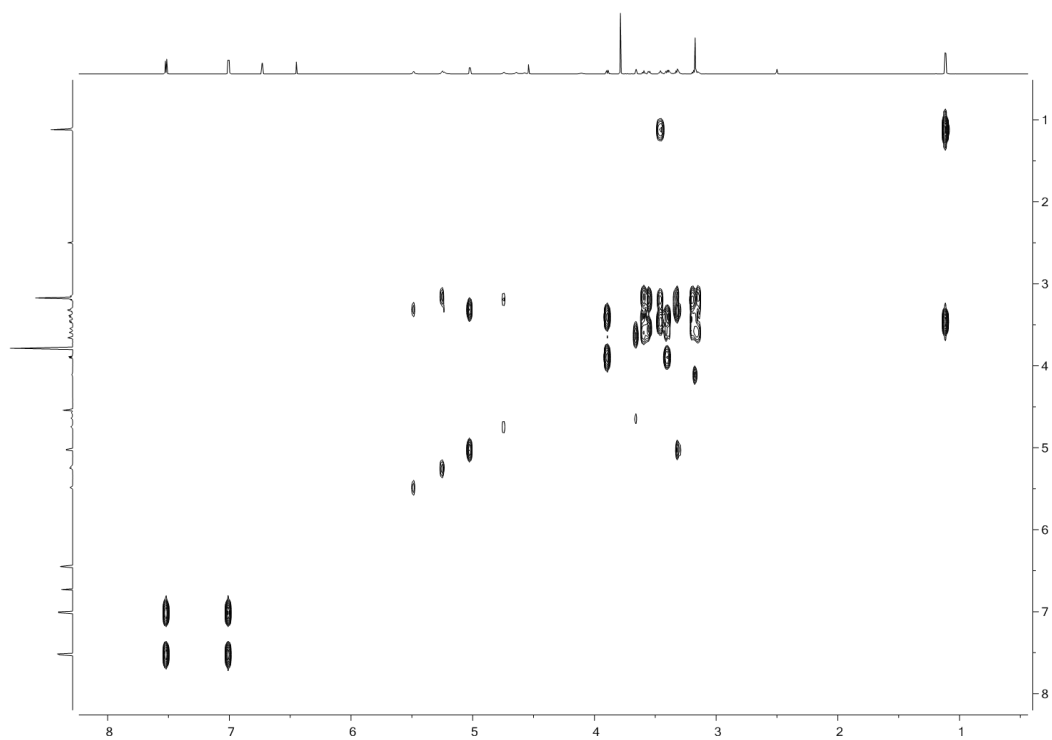


**Fig. 26S** gCOSY spectrum of NP\_592 acquired in DMSO-*d*<sub>6</sub> (800 MHz).

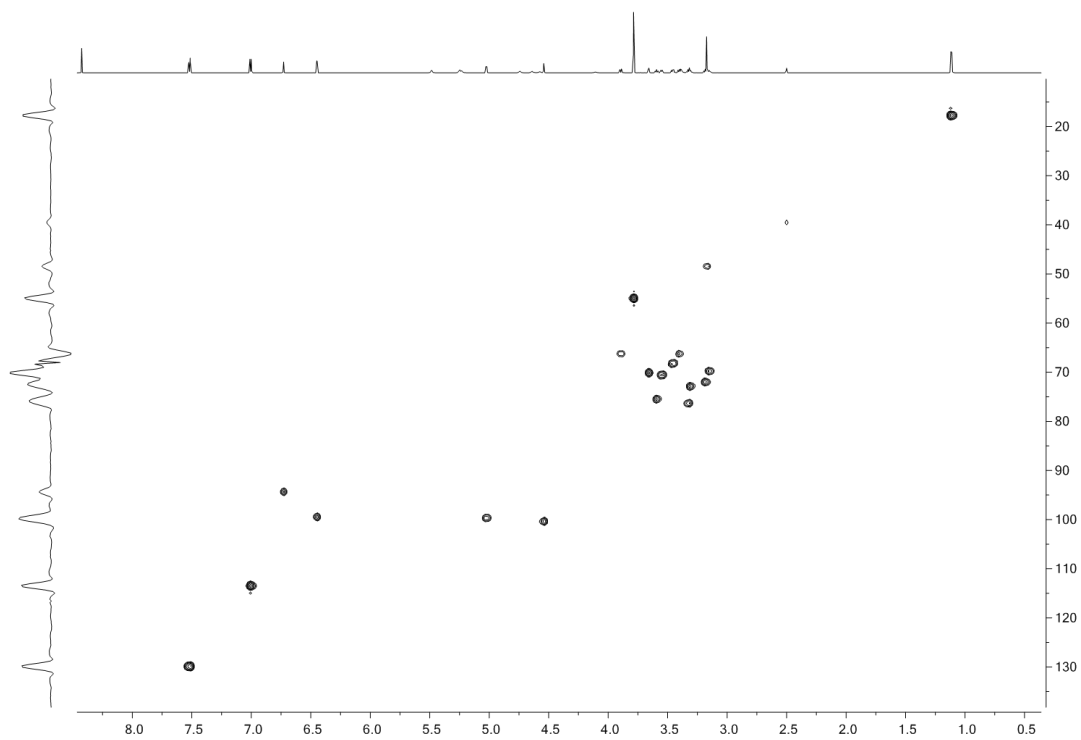


**Fig. 27S** HSQCAD spectrum of NP\_592 acquired in DMSO-*d*<sub>6</sub> (800 MHz).

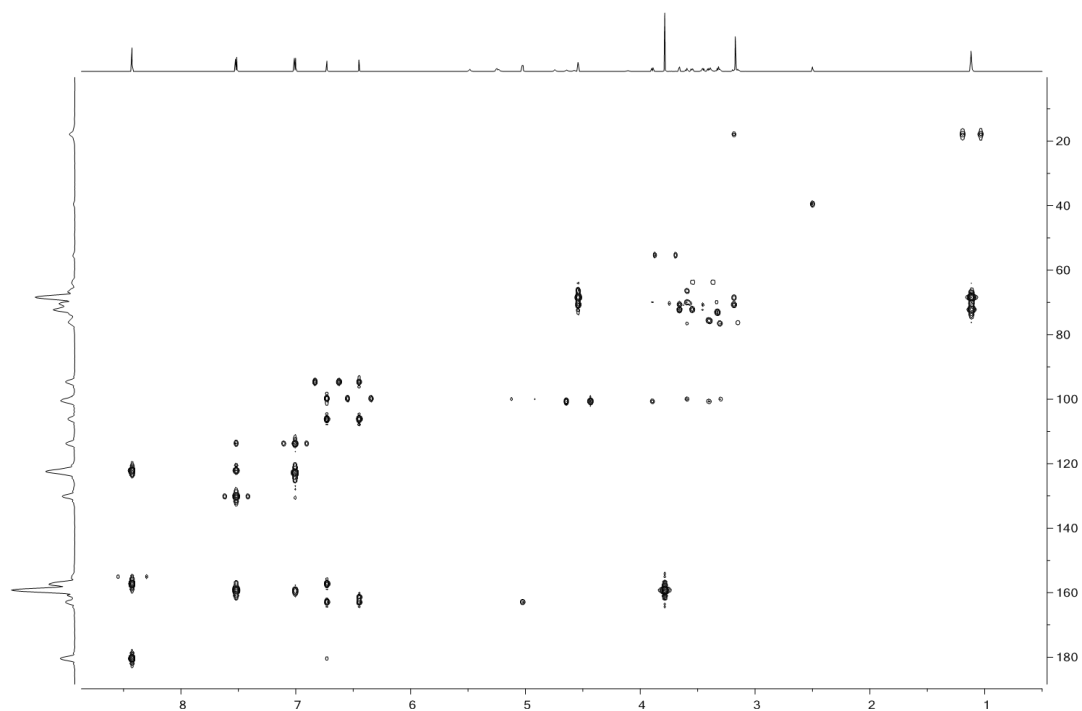


**Fig. 28S** HMBCAD spectrum of NP\_592 acquired in DMSO- $d_6$  (800 MHz).

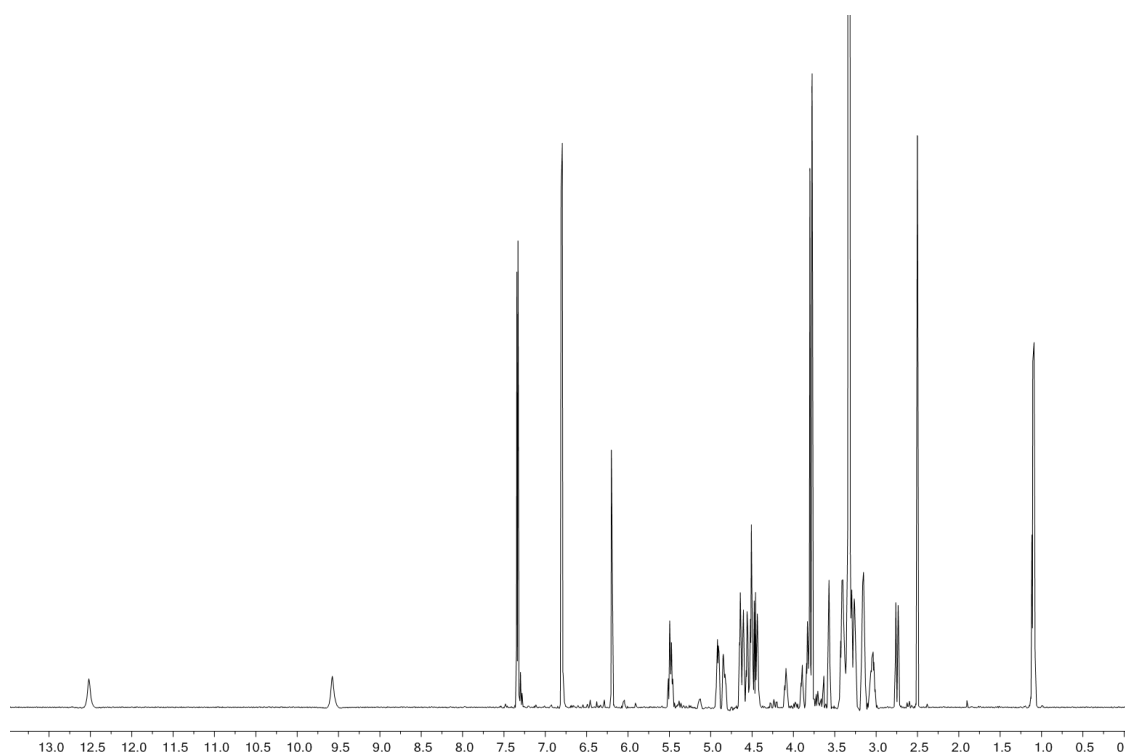


**Fig 29S**  $^1\text{H}$ -NMR spectrum of NP\_594 acquired in DMSO- $d_6$  (800 MHz).



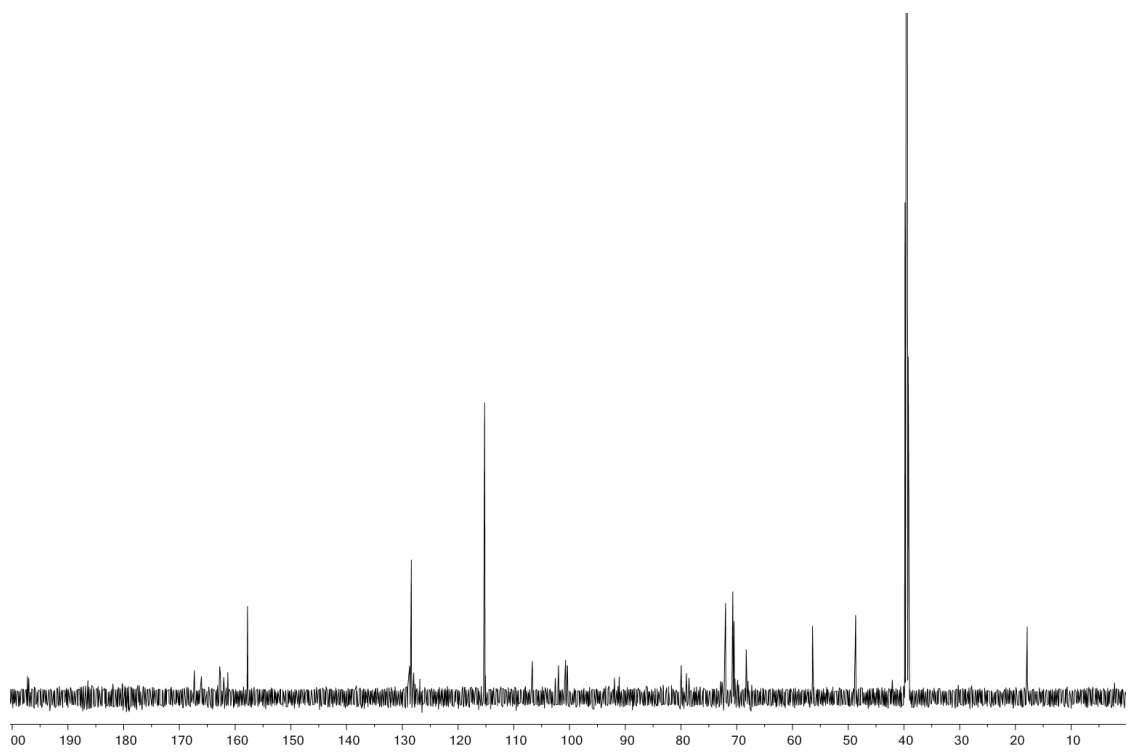


**Fig. 30S**  $^{13}\text{C}$ -NMR spectrum of NP\_594 acquired in  $\text{DMSO-}d_6$  (800 MHz).

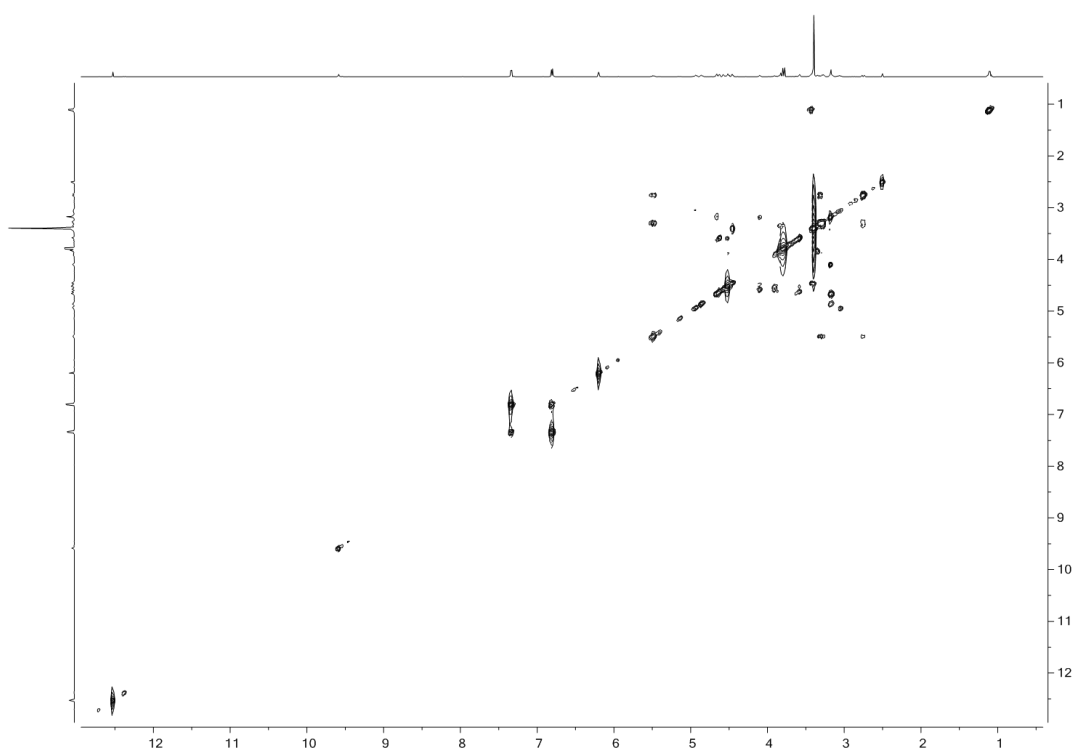


**Fig. 31S** gCOSY spectrum of NP\_594 acquired in  $\text{DMSO-}d_6$  (800 MHz).

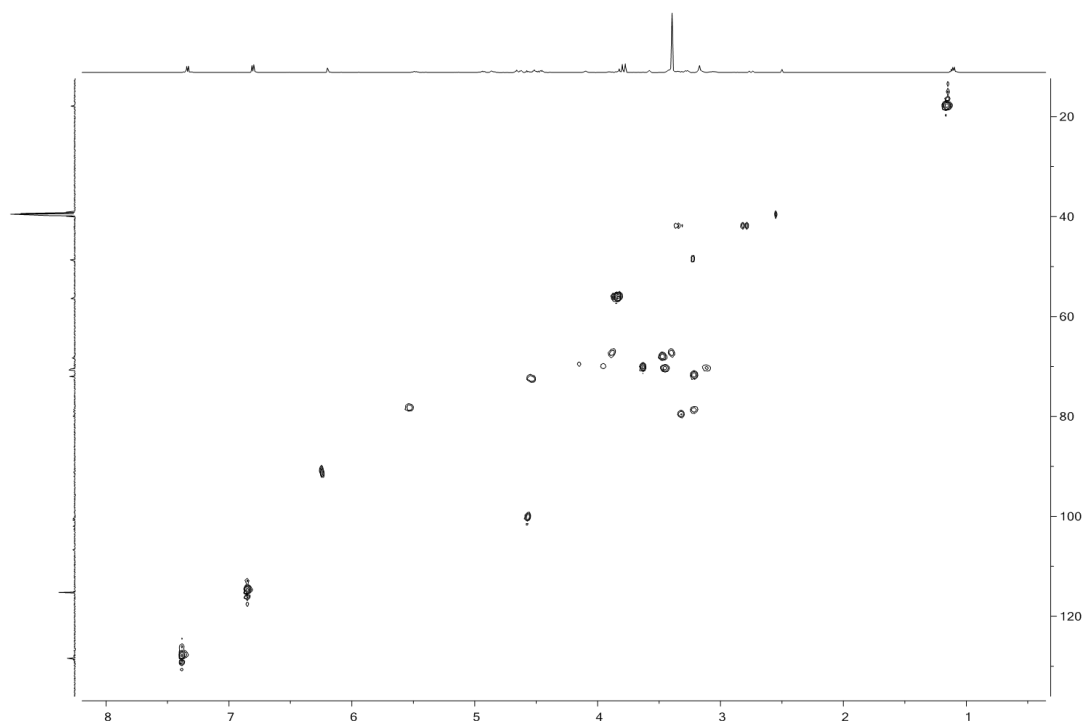


**Fig. 32S** HSQCAD spectrum of NP\_594 acquired in DMSO- $d_6$  (800 MHz).

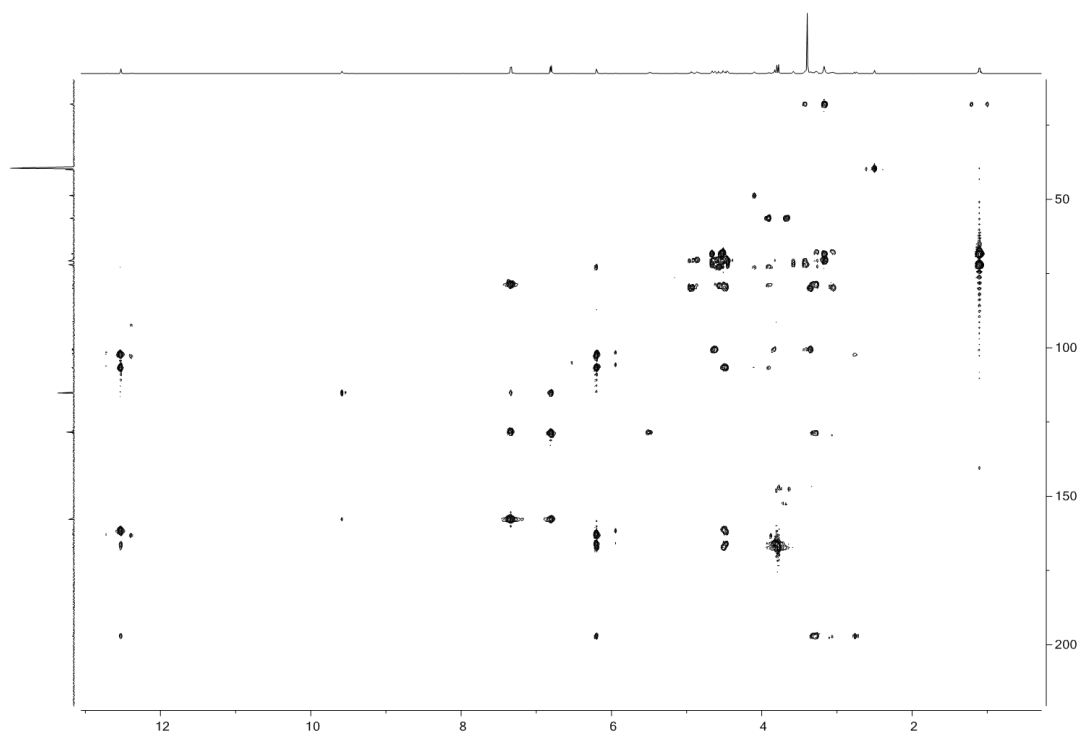


**Fig. 33S** HMBCAD spectrum of NP\_594 acquired in DMSO- $d_6$  (800 MHz).

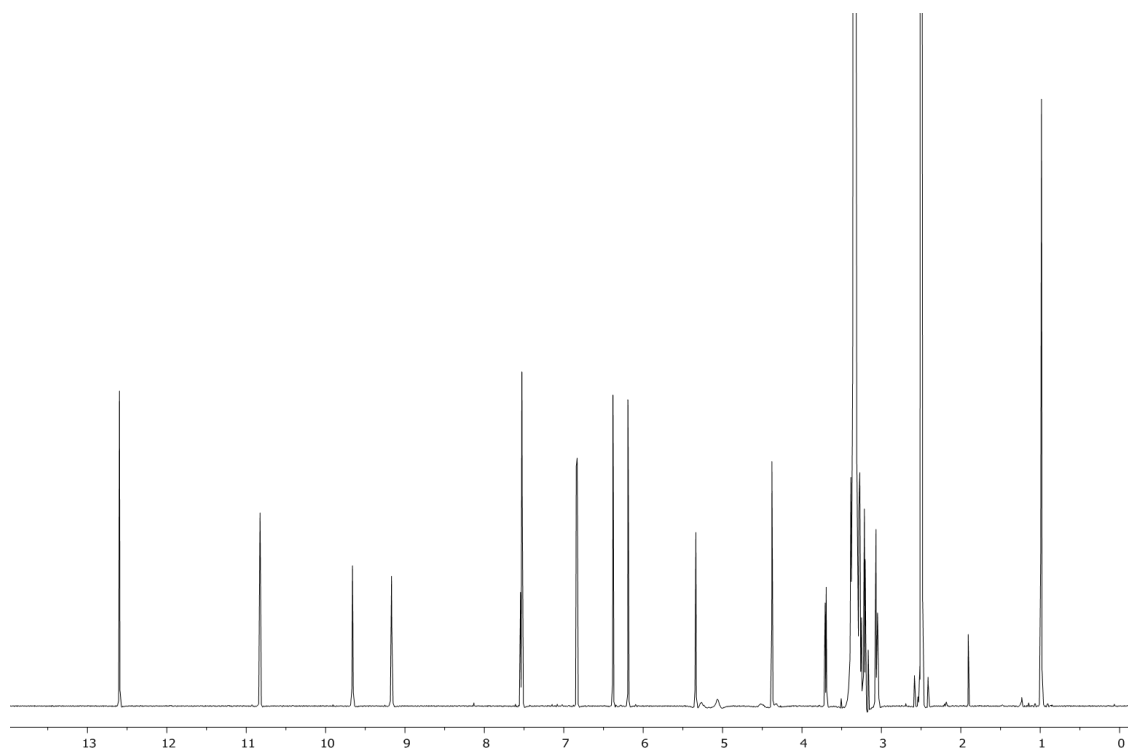


**Fig. 34S**  $^1\text{H-NMR}$  spectrum of NP\_610 acquired in  $\text{DMSO-}d_6$  (800 MHz).

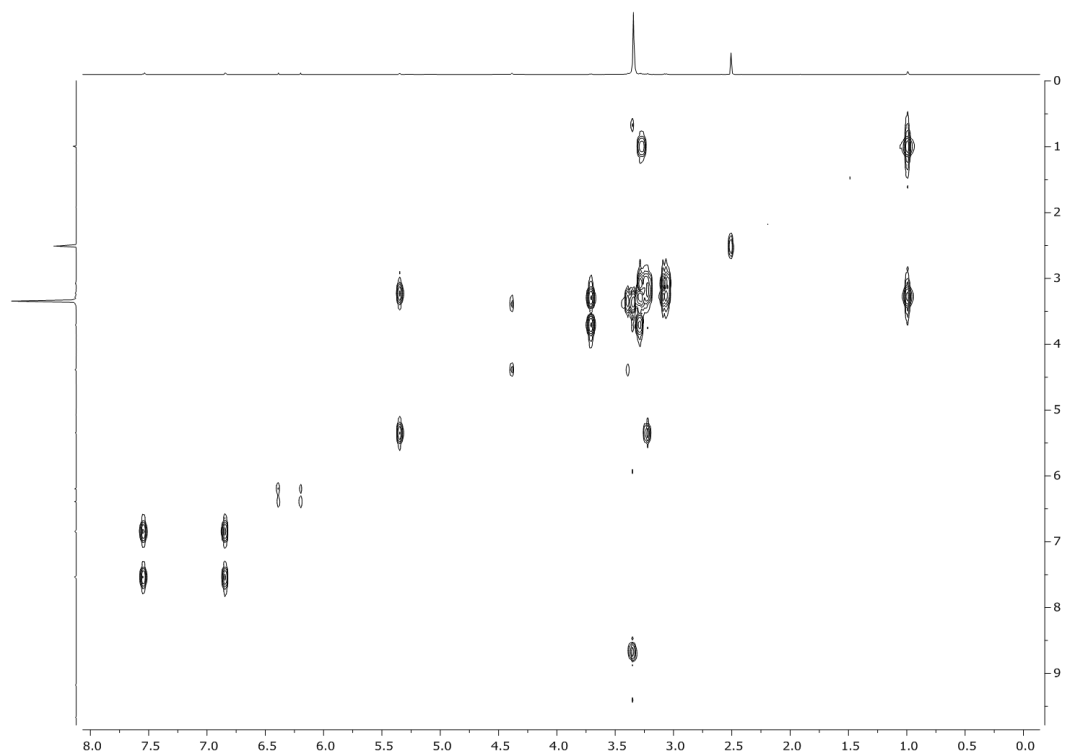


**Fig. 35S** gCOSY spectrum of NP\_610 acquired in  $\text{DMSO-}d_6$  (800 MHz).

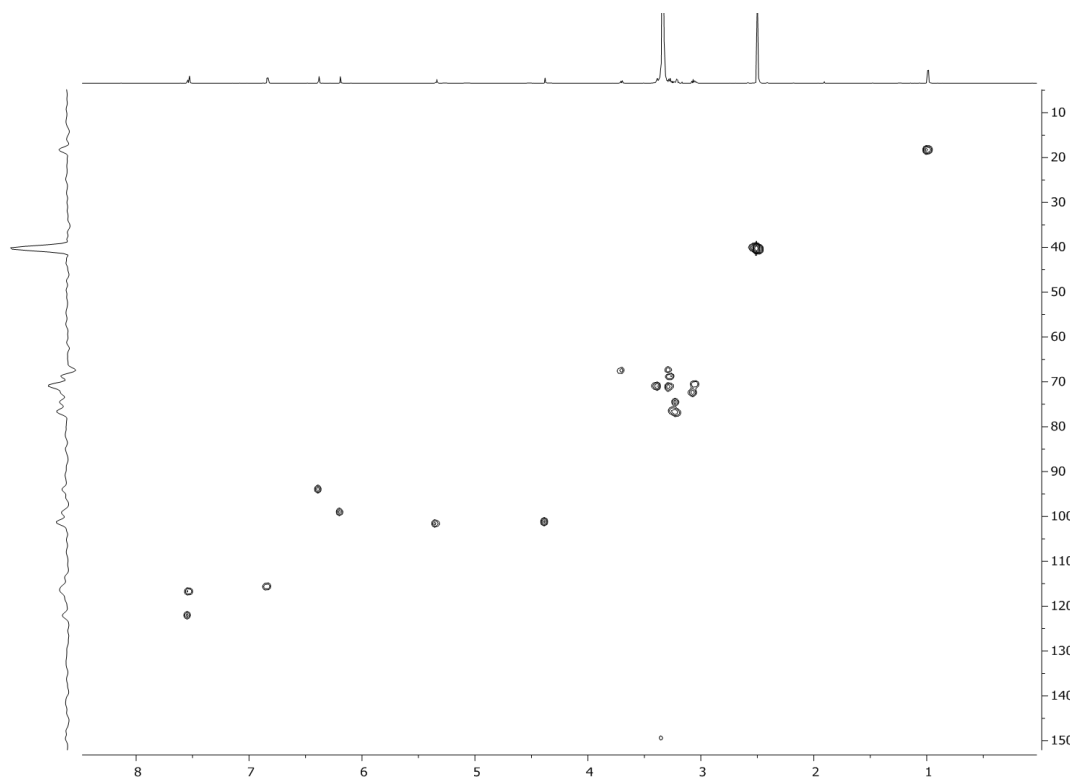


**Fig. 36S** HSQCAD spectrum of NP\_610 acquired in DMSO- $d_6$  (800 MHz).

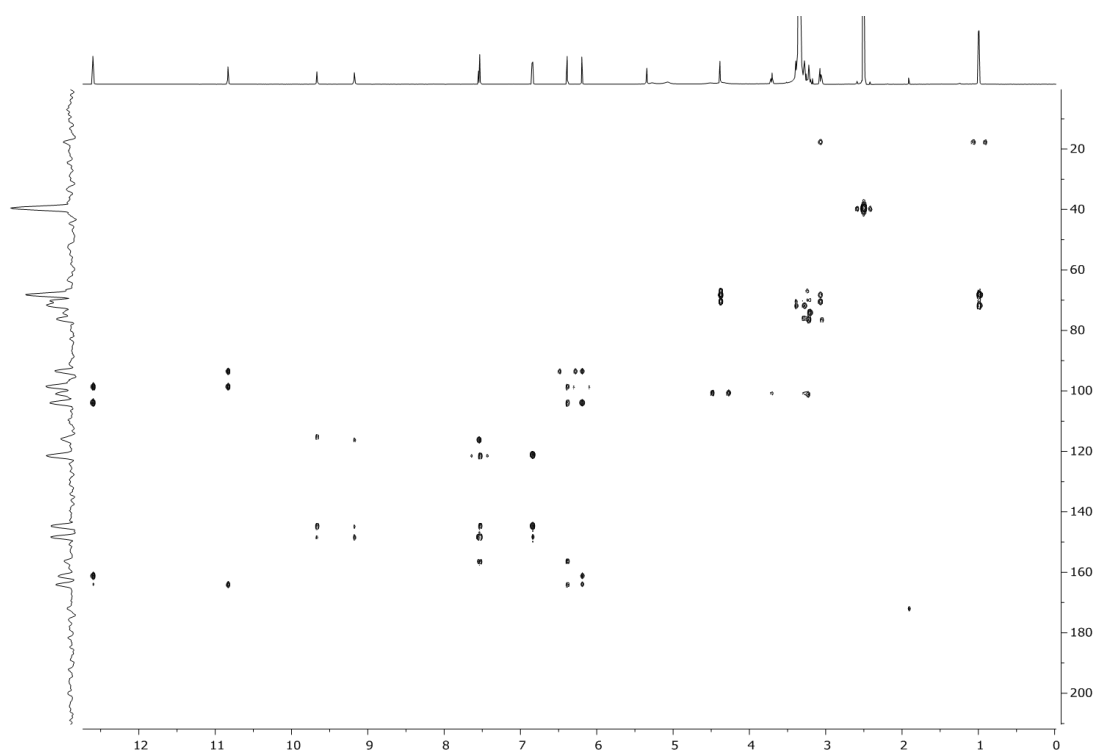


**Fig. 37S** HMBCAD spectrum of NP\_610 acquired in DMSO- $d_6$  (800 MHz).

**Table 1S** The amino acid sequences of the proteins that were used for the screening of natural products.

Protein	Sequence
Human S100A4	ACPLEKALDVMVSTFHKYSGKEGDKFKLNKSELKELLTRELPSFLG KRTDEAAFQKLMSNLDSNRDNEVDFQEYCVFLSCIAMMCNEFFEG FPDKQPRKK
Mouse TIM3	MDGYKVEVGKNAYLPCSYTLPTSGTLVPMCWGKGFCPWSQCTNE LLRTDERNVTYQKSSRYQLKGDNLKGDVSLIKNVTLDDHGTYCC RIQFPGLMNDKKLELKLDIK
Human TIGIT	MMTGTIETTGNISAEEKGGSILQCHLSSTTAQVTQVNWEQQDQLLAI CNADLGWHISPSFKDRVAPGPGLGLTLQSLTVNDTGEYFCIYHTYP DGTYTGRIFLEVLESSVAEHGAR

**Table 2S** Base intensities of the proteins in different concentrations.

Protein	Dilution ( $\mu$ M)	<sup>¥</sup> Absolute intensity
S100A4 /	87.4	5385071.566
S100A4-Ca <sup>2+</sup>	17.5*	3238729.667
	3.5	2758871.333
TIM3	79.5	6345214.356
	15.9*	3395112.630
	3.2	864610.564
TIGIT	69.1	21167179.563
	13.8*	30268892.365
	2.7	246100.5642

<sup>¥</sup>Average intensity of 10 replicates; \*Optimum concentration for ESI-FTMS screening

**Table 3S** Gradient timetable for lead-like enhanced fractionations.

No.	Time (min)	Flow (mL/min)	% B	% C
1	0.01	4.00	10.0	90.0
2	3.00	4.00	50.0	50.0
3	3.01	3.00	50.0	50.0
4	6.50	3.00	100.0	0.0
5	7.00	3.00	100.0	0.0
6	7.01	4.00	100.0	0.0
7	8.00	4.00	100.0	0.0
8	9.00	4.00	10.0	90.0
9	11.00	4.00	10.0	90.0

B: 0.1% Trifluoroacetic acid in methanol

C: 0.1% Trifluoroacetic acid in water

**Table 4S** Optimum conditions for critical instrumental parameters in Bruker Apex III 4.7 Tesla in the positive ESI mode.

Source parameter	Screening conditions
Sample flow rate ( $\mu\text{L/h}$ )	120
Drying gas flow rate (L/min)	40
Drying gas temperature ( $^{\circ}\text{C}$ )	125
Nebulizer gas pressure (psi)	50
Capillary voltage (V)	-5000
End Plate voltage (V)	-3500
Capillary exit voltage (V)	100
Skimmer 1 (V)	24.5
Skimmer 2 (V)	24.0
Hexapole RF amplitude (Hz)	600
Hexapole DC offset (V)	1.5
Hexapole accumulation time (s)	3
Tripple voltage (V)	23
Excitation voltage (V)	-10

**Table 5S** Optimum conditions for critical instrumental parameters in Bruker SolariX 12 Tesla in the positive ESI mode.

Instrumental parts	Parameters	Screening conditions
Syringe pump	Sample Flow rate ( $\mu\text{L/h}$ )	120
API source	Capillary (V)	-4500
	End plate off set (V)	-1000
Source gas tune	Nebulizer (bar) <sup>t</sup>	1-2
	Dry gas (L/min) <sup>t</sup>	4-6
	Dry gas temperature ( $^{\circ}\text{C}$ ) <sup>m</sup>	120-200
Ion transfer		
Source optics	Capillary exit (V)	220.0
	Deflector plate (V)	250.0
	Funnel 1 (V) <sup>t</sup>	*110.0-150
	Skimmer 1 (V) <sup>t</sup>	*15.0-30.0
	Funnel RF Amplitude (Vpp)	250.0
Octopole	Frequency (MHz) <sup>m</sup>	2-5
	RF amplitude (Vpp)	200.0
Quadrupole	Q1 mass ( $m/z$ )	600.0
Collision cell	Collision Cell (V)	-3.0
	DC Extracts Bias (V)	0.1
	RF Frequency (MHz)	2
	Collision RF Amplitude (Vpp)	2000.0
Transfer optics	Time of Flights (ms) <sup>t</sup>	1.500-2.500
	Frequency (MHz)	2
	RF amplitude (Vpp)	450.0
Magnitude	Size <sup>t</sup>	1-2M
	Mass range <sup>m</sup>	294.85-10000.00
	Average scans / number of scans <sup>a</sup>	16-64
	Accumulation time (s) <sup>t</sup>	0.7-1.5

Screening conditions were varied during: <sup>t</sup> tuning for the proteins or samples, <sup>m</sup> method setup for the proteins, <sup>a</sup> acquisition of the sample spectra

**Table 6S** Gradient timetable for LC-HRMS analysis of extracts.

No.	Time (min)	Flow (mL/min)	% B	% C
1	0.01	1.00	5.0	95.0
2	2.50	1.00	5.0	95.0
3	16.0	1.00	100.0	0.0
4	18.0	1.00	100.0	0.0
5	20.0	1.00	5.0	95.0

B: 0.1% Formic acid in methanol  
C: 0.1% Formic acid in water

**Table 7S** Optimum conditions for critical instrumental parameters of Bruker MaXis II OTOF in the positive ESI mode.

Instrument parameters		Optimum conditions
Source	End Plate Offset (V)	-450
	Capillary (V)	-4500
	Nebulizer (Bar)	1.0
	Dry Gas (L/min)	5.0
	Dry temperature (°C)	120
Tune		
Transfer	Funnel 1 RF (Vpp)	-15.0
	isCID energy (eV)	0.0
	Multiple RF (Vpp)	-110.0
Quadrupole	Ion Energy (eV)	-0.1
	Low Mass ( $m/z$ )	80
Collision cell	Collision (eV)	-5.0
	Collision RF (Vpp)	-500.0
	Transfer time ( $\mu$ s)	100.0
	Pre Pulse Storage ( $\mu$ s)	5.0



**Table 8S** Charge deconvolution parameters used for LC-HRMS analysis of extracts.

Parameters	Deconvolution conditions (+ESI, MS)
Adduct ions	[M + H] <sup>+</sup> , [M + Na] <sup>+</sup>
Mass range ( <i>m/z</i> )	250-4000
Abundance cutoff (%)	2.5
Maximum charge	Auto
Signal-to-noise ratio	4

**Table 9S** Gradient timetable for LC-LRMS analysis of extracts.

No.	Time (min)	Flow (mL/min)	% B	% C
1	0.01	1.00	5.0	95.0
2	1.00	1.00	5.0	95.0
3	10.0	1.00	100.0	0.0
4	11.0	1.00	100.0	0.0
5	12.0	1.00	5.0	95.0

B: 0.1% Formic acid in methanol  
C: 0.1% Formic acid in water